Magnetic excitations in the geometrically frustrated pyrochlore antiferromagnet $Gd_2Sn_2O_7$ studied by electron spin resonance

S. S. Sosin
P. L. Kapitza Institute for Physical Problems, RAS, 119334 Moscow, Russia and Commissariat à l'Energie Atomique, DSM/INAC/SPSMS, 38054 Grenoble, France

L. A. Prozorova
P. L. Kapitza Institute for Physical Problems, RAS, 119334 Moscow, Russia

P. Bonville
Commissariat à l'Energie Atomique, DSM/IRAMIS/SPEC, 91191 Gif sur Yvette, France

M. E. Zhitomirsky
Commissariat à l'Energie Atomique, DSM/INAC/SPSMS, 38054 Grenoble, France
(Received 4 September 2008; revised manuscript received 30 October 2008; published 14 January 2009)

The spin dynamics in the geometrically frustrated pyrochlore antiferromagnet $Gd_2Sn_2O_7$ is studied by means of the electron spin resonance. In the ordered phase ($T_N=1$ K), we have detected three gapped resonance modes. Their values agree well with the developed spin-wave theory which takes into account the Heisenberg nearest-neighbor exchange, the single-ion anisotropy, and the long-range dipolar interactions. The theory also predicts a fourth lowest-frequency gap, which lies beyond the experimental range of frequencies, but determines the exponential decrease in the specific heat at low temperature.

DOI: 10.1103/PhysRevB.79.014419 PACS number(s): 75.30.Sg, 75.50.Ee

I. INTRODUCTION

The geometrically frustrated Heisenberg antiferromagnet on a pyrochlore lattice has an extensive degeneracy of the ground state.[1] As a result, weak additional interactions play a prominent role leading to a multitude of magnetic phases and phenomena. A typical example is provided by $Gd_2Sn_2O_7$ and $Gd_2Ti_2O_7$, two pyrochlore antiferromagnets with close values of the nearest-neighbor exchange constants, which, nevertheless, have different-ordered magnetic structures. While the antiferromagnetic ordering in $Gd_2Ti_2O_7$ is resolved on the assumption of a complicated four-wave-vector order parameter with the basic $\mathbf{q}=(1/2,1/2,1/2)$,[2] the second material $Gd_2Sn_2O_7$ has a much simpler four-sublattice spin structure with $\mathbf{q}=0$.[3]

An exponential decrease in the low temperature specific heat of $Gd_2Sn_2O_7$ was recently found by the calorimetric measurements.[4] This result unambiguously points at a gapped excitation spectrum in the ordered magnetic phase. It is somewhat unexpected in view of the results of analogous measurements for $Gd_2Ti_2O_7$,[5] which yield a power-law behavior $C \propto T^2$ down to temperatures on the order of 100 mK. The presence of nonfrozen magnetic degrees of freedom at very low temperature was also related to the persistent spin dynamics observed via the muon spin relaxation (μSR) in $Gd_2Ti_2O_7$ (Refs. 5 and 6) and via Mössbauer[7] and μSR measurements[8,9] in $Gd_2Sn_2O_7$. The observed difference in the low-temperature dependence of the specific heat in the two pyrochlore antiferromagnets must be further corroborated by a direct investigation of the excitation spectrum. Since inelastic neutron-scattering measurements are hindered in Gd compounds, the most convenient experimental technique left is the electron spin resonance (ESR). An absorption of photons with a typical wavelength on the order of $\lambda \sim 1$ cm provides a high-resolution probe of low-energy excitations. For the most probable single photon-magnon process only magnons with small wave vectors $k \sim 1/\lambda \to 0$ can be excited.

Our previous measurements of the ESR spectra in $Gd_2Sn_2O_7$ were performed at temperatures between 10 K (the Curie-Weiss constant is $|\theta_{CW}| \simeq 9$ K) and the ordering transition at $T_N=1$ K.[10] This temperature range is characterized by strong spin correlations in the absence of an order parameter, which is commonly called a cooperative paramagnet. An unusual transformation of an exchanged narrowed paramagnetic line into a single gapped resonance mode with linear field dependence was observed in this regime.

The present work investigates further transformations of the resonance spectrum at temperatures below the magnetic ordering transition. Three gapped modes are observed, two of which are degenerate in zero magnetic field. The gap values are reproduced by the spin-wave calculations using the known values of the exchange constant, the dipolar, and the single-ion anisotropy energies. The fourth gap predicted by the theory remains unobserved in our experimental range but agrees well with the specific-heat data.

II. SAMPLES

Powder samples of $Gd_2Sn_2O_7$ were prepared by the method described in a previous publication.[11] For sample characterization we have measured the specific heat in a ^{3}He-^{4}He dilution fridge in the temperature range of 0.1–2 K. The data are obtained using a quasiadiabatic technique with continuous heating of the sample.[12] In order to improve the

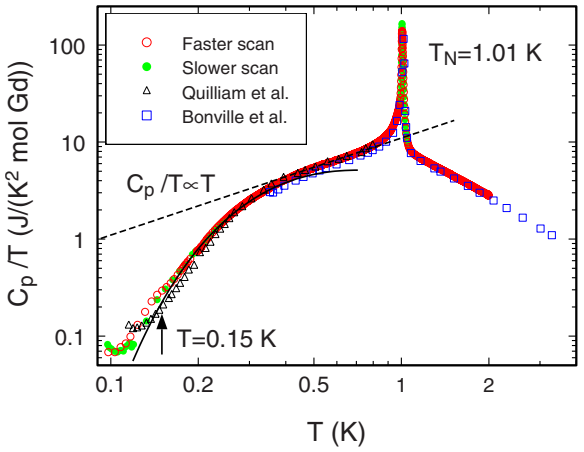

FIG. 1. (Color online) Thermal variation in the specific heat divided by temperature in $Gd_2Sn_2O_7$ measured with different heating rates (● and ○ are faster and slower scans, respectively); □ and △ are previous data from Refs. 4 and 11; the dashed line is a linear approximation to the high-temperature part of the data, the fit by a solid line is described in the text, and the arrow marks the low-temperature limit of data reliability.

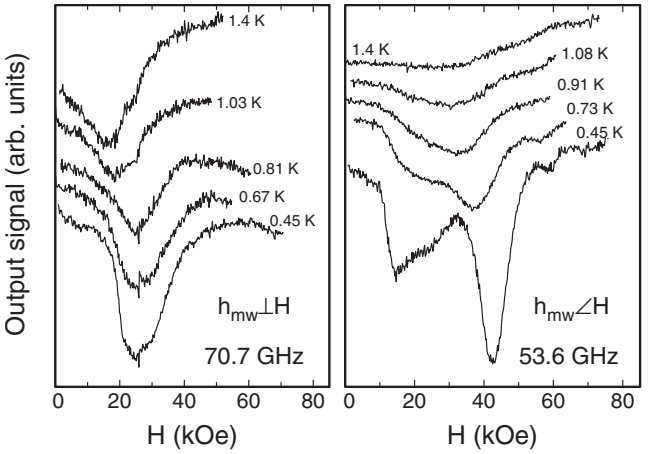

FIG. 2. Evolution of the magnetic-resonance absorption spectra in a powder sample of $Gd_2Sn_2O_7$ on cooling from above the ordering transition to T=0.45 K recorded in a perpendicular polarization of the microwave field with respect to the external field $\mathbf{h}_{mw} \perp \mathbf{H}$ (left panel) and in a tilted polarization (right panel); the recorded lines are shifted upwards for clarity.

thermal contact between the insulating powder sample and the sample holder, 1.5 mg of the powder was mixed with 1 mg of Apiezon N grease, wrapped into a silver foil, and pressed. The quality of the thermal contact has been verified by comparing the data obtained in experiments with different heating rates. The range of fully reliable results corresponds to temperatures above 0.15 K.

Our experimental results for the specific heat are presented in Fig. 1. Two subsequent temperature scans shown by open and closed circles (slower and faster scans, respectively) are in satisfactory agreement with each other. A sharp peak is observed at the ordering transition with T_N=1.01 K. The previously published data[11] obtained with the same measurement technique are shown by squares and lie 5%–10% lower in the whole range of temperatures. This systematic discrepancy is probably associated with a different quality of thermal contacts in both experiments. The measurements from Ref. 4 (triangles) demonstrate a perfect agreement with our data above 0.4 K, where both curves can be empirically fitted by a $C \propto T^2$ dependence. Both sets of data also agree but less perfectly below 0.4 K and show a drastic decrease in cooling. According to our measurements, the most significant reduction in the specific heat (by a factor of 20) occurs in the temperature interval of 0.3–0.15 K. Decreasing temperature further down to 0.1 K leads to an additional specific-heat reduction by a factor of 5 to the level, which does not exceed the experimental accuracy. The specific heat decreases faster than any reasonable power law T^n, which suggests an exponential temperature dependence in agreement with the theoretical prediction of Ref. 13 and with the previous experimental study.[4]

III. MAGNETIC RESONANCE

Magnetic-resonance measurements have been carried out in a transmission-type spectrometer with a cylinder cavity designed for frequencies above 25 GHz, which was equipped with a ^{3}He cryostat with a minimum working temperature of 0.4 K. The magnetic field up to 100 kOe is generated by a cryomagnet. The absorption spectra are recorded on forward and backward field sweeps.

To start with, we have traced the evolution of the resonance absorption lines on cooling the sample from the strongly correlated disordered state through the ordering transition at T_N=1.0 K down to the lowest experimental temperature (0.45 K) at which the system is fully ordered (the magnetic transition is first order[11]). Two sets of measurements with different polarizations of the microwave field with respect to the external magnetic field were performed. The left panel of Fig. 2 shows the resonance spectra of a sample glued onto the bottom of the cavity where the microwave field has only a component perpendicular to the external field $\mathbf{h}_{mw} \perp \mathbf{H}$. The single resonance line observed at all frequencies for $T > T_N$ changes its shape and shifts to larger fields when going through the transition. This shift results from an unusual linear field dependence of the resonance gap in the cooperative paramagnetic state, as discussed in Ref. 10.

The absorption spectra are significantly modified when the sample is placed into a microwave field with a component along the external field. Additional lines develop in the spectrum below 1 K, one of them having a much larger intensity than the others. The properties of all these resonance modes were studied in detail at the lowest experimental temperature 0.45 K.

The upper panel of Fig. 3 shows the resonance spectra for a sample with $\mathbf{h}_{mw} \perp \mathbf{H}$. These data have been briefly discussed before.[14] The single resonance lines observed at various frequencies belong to two different branches, one of which is decreasing (line A) and the other one is increasing (line B) in field. The extrapolation of these lines to zero field gives the same gap value of 33.5 ± 0.5 GHz (1.61 ± 0.02 K) for both branches, which points to an exact degeneracy of the

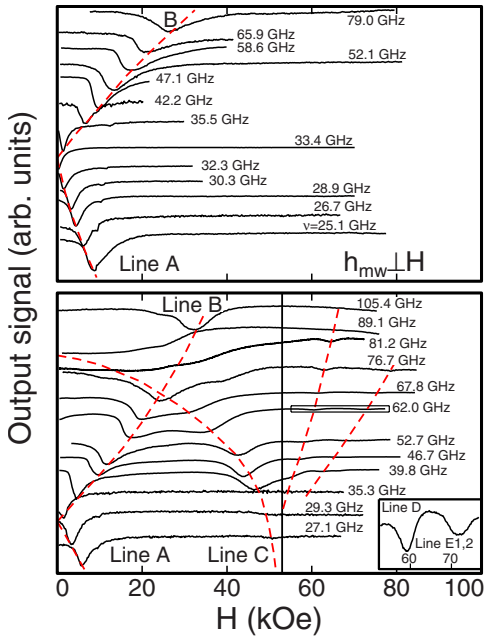

FIG. 3. (Color online) The magnetic-resonance absorption spectra in a powder sample of $Gd_2Sn_2O_7$ recorded at $T=0.45$ K for various frequencies with $\mathbf{h}_{mw} \perp \mathbf{H}$ (upper panel) and in a tilted direction of $\mathbf{h}_{mw}$ (lower panel); dashed lines are guide for the eyes in tracing the field evolution of different resonance lines labeled by letters A–E; the inset in the lower panel expands the in-frame part of the absorption record at $\nu=62.0$ GHz including spectral lines D and E. The second-order transition at $H_s=53$ kOe is marked by a vertical line.

corresponding magnetic excitations. No other resonance absorption was detected within the experimental accuracy of 0.5%.

The absorption spectra obtained for a tilted direction of $\mathbf{h}_{mw}$ are presented on the lower panel of Fig. 3. The intense sharp resonance line shown in Fig. 2, which arises in the ordered phase, appears to be a third branch with a gap of 85 ± 5 GHz (4.1 ± 0.2 K, line C). This mode decreases with increasing magnetic field and softens in the vicinity of the continuous second-order transition. Extrapolating its field dependence to zero frequency, one can determine the value of the critical field $H_s=53.0 \pm 0.5$ kOe. This transition is associated with the lowering of the symmetry of the magnetic structure but not exactly coincides with the saturation field. Due to anisotropy effect, the collinear phase should be reached at a larger field. According to experimental estimations of Ref. 10 the full saturation of the magnetic moment occurs at a field of about 58 kOe. A careful study of the spectrum above the critical field again reveals the existence of three weak components (line D and double split line E) increasing in field, with line E doublet exhibiting an exact linear field dependence.

Our ESR measurements directly detect three resonance modes in zero magnetic field. Two of them (lines A and B) are exactly degenerate with a gap of $\Delta_{2,3}=1.61$ K and the third mode has a larger gap of $\Delta_4=4.1$ K. In addition, the previous specific-heat measurements and theoretical calculations suggest the presence of a fourth lowest branch at energy $\Delta_1 \sim 1.2$ K.[4,13] The corresponding frequency $\nu_1 \sim 25$ GHz lies near the lower boundary of our experimentally accessible range. Hence, it is natural that this mode remains unobserved in the ESR experiment provided that it decreases with increasing magnetic field. A crude estimate from the low-T fit of our specific-heat data $C(T) \propto T^{-1/2} e^{-\Delta/T}$ (the corresponding fit is shown by the solid line in Fig. 1) also gives $\Delta_1 \sim 1.0$ K. One should note here that more elaborate fits at temperatures below 0.15 K (including, e.g., nuclear contributions) would rely on an overestimation of the experimental accuracy due to the degradation of the thermal contact in insulating powder samples in this temperature range. Very recently, inelastic neutron measurements[15] on a powder sample of $Gd_2Sn_2O_7$ reveal a few gapped excitation modes in the range of 0.1–0.5 meV in full agreement with our results.

The previous spin-wave calculations[13] reflect the general features of the measured spectrum, with a 10%–20% accuracy for the observed gaps. The principal qualitative difference with our work is that our ESR measurements find two *exactly* degenerate magnon branches at $\mathbf{k}=0$ in zero magnetic field, whereas Ref. 13 predicts a finite splitting between them: $\Delta_2=1.76$ K and $\Delta_3=1.93$ K. In Sec. IV we present the detailed theoretical calculations of the ESR spectra in $Gd_2Sn_2O_7$, which not only yield the correct degeneracy of $\mathbf{k}=0$ magnons but also show an overall improved agreement with the experimental data.

IV. SPIN-WAVE THEORY

The unit cell of the pyrochlore lattice contains four magnetic atoms. Their positions and the specific choice of the local axes adopted below are

$$\boldsymbol{\rho}_1 = (0,0,0), \quad \hat{\mathbf{z}}_1 = \frac{1}{\sqrt{2}}(1,-1,0),$$

$$\boldsymbol{\rho}_2 = \left(0,\frac{1}{4},\frac{1}{4}\right), \quad \hat{\mathbf{z}}_2 = \frac{1}{\sqrt{2}}(-1,-1,0),$$

$$\boldsymbol{\rho}_3 = \left(\frac{1}{4},0,\frac{1}{4}\right), \quad \hat{\mathbf{z}}_3 = \frac{1}{\sqrt{2}}(1,1,0),$$

$$\boldsymbol{\rho}_4 = \left(\frac{1}{4},\frac{1}{4},0\right), \quad \hat{\mathbf{z}}_4 = \frac{1}{\sqrt{2}}(-1,1,0), \tag{1}$$

with $\hat{\mathbf{y}}_i \equiv (0,0,1)$ and $\hat{\mathbf{x}}_i = \hat{\mathbf{y}}_i \times \hat{\mathbf{z}}_i$. The unit cell tetrahedra form a face-centered-cubic structure with the translational basis $\mathbf{a}_1=(0,\frac{1}{2},\frac{1}{2})$, $\mathbf{a}_2=(\frac{1}{2},0,\frac{1}{2})$, and $\mathbf{a}_3=(\frac{1}{2},\frac{1}{2},0)$.

In the following we will take into account all major magnetic interactions starting with the strongest nearest-neighbor exchange:

$$\hat{\mathcal{H}} = J \sum_{\langle ni,mj \rangle} \mathbf{S}_{ni} \cdot \mathbf{S}_{mj}, \tag{2}$$

where n and m denote unit cells and i and $j=1-4$ indicate position inside cell. The equilibrium magnetic structure de-

termined for $Gd_2Sn_2O_7$ in neutron-diffraction experiments[3] is a four-sublattice chiral spin cross with $\mathbf{S}_i \| \hat{\mathbf{z}}_i$, which is also known as the Palmer-Chalker state.[16] This state is one out of the many degenerate spin structures obeying the classical constraint: $\Sigma_i \mathbf{S}_i = 0$ for every tetrahedron, which must be fulfilled by the ground state in the absence of single-ion anisotropy and dipolar interactions.

Let us first calculate the excitation spectrum for the chiral spin-cross state neglecting all magnetic anisotropies. The local coordinate system is used for the spin operators $\mathbf{S}_i = S_i^x \hat{\mathbf{x}}_i + S_i^y \hat{\mathbf{y}}_i + S_i^z \hat{\mathbf{z}}_i$, where the three axes are defined above [Eq. (1)]. Since we are dealing with the $\mathbf{k}=0$ magnetic structure, the local axes do not carry the cell index n. The Holstein-Primakoff transformation is used for the bosonic representation of spin operators. Since gadolinium spins $S=7/2$ are large, we neglect interactions between magnons and always keep up with the quadratic terms in the bosonic Hamiltonian. With the chosen accuracy it is sufficient to write

$$S_i^z = S - a_i^\dagger a_i, \quad S_i^x = \sqrt{\frac{S}{2}}(a_i^\dagger + a_i),$$

$$S_i^y = \sqrt{\frac{S}{2}} i (a_i^\dagger - a_i). \tag{3}$$

The obtained quadratic form is diagonalized by performing consecutively Fourier and Bogoliubov transformations. The excitation spectrum consists of four branches,

$$\varepsilon_{1,2}(\mathbf{k}) \equiv 0, \quad \varepsilon_{3,4}(\mathbf{k}) = 2JS\sqrt{1 - \cos\frac{k_x}{2}\cos\frac{k_y}{2}}. \tag{4}$$

Two of them have zero energy everywhere in the Brillouin zone, which reflects the infinite degeneracy of the nearest-neighbor exchange Hamiltonian on a pyrochlore lattice. Interestingly, the two other branches have purely two-dimensional (2D) dispersions in the harmonic approximation. Various perturbations to the nearest-neighbor Heisenberg Hamiltonian [Eq. (2)] should produce a finite dispersion of the two lowest branches, but the quasi-2D behavior of $\varepsilon_{3,4}(\mathbf{k})$ for the two higher-energy modes should survive in a certain range of parameters.

As the next step we add the single-ion anisotropy to Eq. (2) in the form of the lowest-order crystal-field harmonics

$$\hat{\mathcal{H}}_a = D_a \sum_i (\mathbf{S}_i \cdot \mathbf{n}_i)^2, \tag{5}$$

with $\mathbf{n}_i$ being the four local anisotropy axes parallel to the principal cubic diagonals. Keeping again only quadratic terms in the bosonic representation one obtains

$$(\mathbf{S}_i \cdot \mathbf{n}_i)^2 = S\left(a_i^\dagger a_i + \frac{1}{2}\right) + \frac{S}{6}[a_i^2(1 \pm 2\sqrt{2}i) + a_i^{\dagger 2}(1 \mp 2\sqrt{2}i)], \tag{6}$$

where the upper (lower) sign corresponds to $i=1,4$ (2,3).

Since we are interested in the ESR spectrum given by $\mathbf{k}=0$ magnons, we simplify the following calculations by considering only uniform modes, avoiding hence a step with the Fourier transformation. The exchange Hamiltonian projected onto the four-site magnetic unit cell is written as

$$\begin{aligned}\hat{\mathcal{H}}_1^{(2)}/JSN = {} & 2(a_1^\dagger a_1 + a_2^\dagger a_2 + a_3^\dagger a_3 + a_4^\dagger a_4) + a_1^\dagger(a_2 + a_3) \\ & + a_2^\dagger(a_1 + a_4) + a_3^\dagger(a_1 + a_4) + a_4^\dagger(a_2 + a_3) \\ & - a_1(a_2 + a_3 + 2a_4) - a_2(2a_3 + a_4) - a_3 a_4 + \text{H.c.},\end{aligned} \tag{7}$$

where N is the number of unit cells in the lattice. The single-ion anisotropy is represented as

$$\begin{aligned}\hat{\mathcal{H}}_a^{(2)}/D_a SN = {} & a_1^\dagger a_1 + a_2^\dagger a_2 + a_3^\dagger a_3 + a_4^\dagger a_4 \\ & + \frac{1}{6}(1 - 2\sqrt{2}i)(a_1^2 + a_4^2 + a_2^{\dagger 2} + a_3^{\dagger 2}) + \text{H.c.}\end{aligned} \tag{8}$$

Diagonalization of quadratic forms, with the help of a generalized Bogoliubov transformation, has been described many times in the literature[17] and will not be repeated here. In the present case the diagonalization can be performed analytically, yielding four magnon gap energies

$$\Delta_1 = 0, \quad \Delta_{2,3} = 2S\sqrt{2D_a J/3}, \quad \Delta_4 = 2\Delta_2. \tag{9}$$

The lowest magnon branch remains gapless in spite of the single-ion term. This is in agreement with the analysis of Ref. 18, which finds an infinite (but not extensive) degeneracy for the easy-plane pyrochlore antiferromagnet.

The double degeneracy of the two intermediate magnon modes $\Delta_{2,3}$ follows from the tetragonal symmetry of the chiral spin-cross structure. Analysis of the eigenvectors of the Bogoliubov transformation identifies corresponding oscillations with *out-of-plane* motion of only one pair of spins S_1, S_4 or S_2, S_3 with opposite phases. The two modes transform into each other according to the 2D irreducible representation of the tetragonal point group. Extra interactions (dipolar, etc.) will not modify such a degeneracy as long as the chiral spin-cross structure remains stable. The two other modes $\Delta_{1,4}$ correspond to predominantly *in-plane* motion of all four spins.

For a simple numerical estimate we use the following parameters for $Gd_2Sn_2O_7$: $|\theta_{CW}| = 2JS(S+1) \approx 8.6$ K (Ref. 11) with $J = 2/63|\theta_{CW}| = 0.27$ K and $D_a \approx 0.14$ K.[19] This yields the following values $\Delta_{2,3} = 1.12$ K and $\Delta_4 = 2.24$ K, which are somewhat lower than the experimentally measured frequencies (1.61 and 4.1 K, respectively). Introduction of further neighbor exchanges will not modify the above results: (i) the third-neighbor exchange J_3 (the notation is taken from Ref. 3) couples spins on the same sublattice and, consequently, does not contribute to the $\mathbf{k}=0$ modes; and (ii) the antiferromagnetic second-neighbor exchange J_2 yields the same replacement $J \to J + 2J_2$ in the expressions for θ_{CW} and for the uniform modes and does not, therefore, change the gaps.

The next important perturbation to the exchange energy [Eq. (2)] is the dipole-dipole interaction[13,20]

$$\hat{\mathcal{H}}_{\rm dip} = \frac{D}{2S^2}\sum_{ni,mj}\frac{\mathbf{S}_{ni}\cdot\mathbf{S}_{mj} - 3(\mathbf{S}_{ni}\cdot\mathbf{r}^{ij}_{nm})(\mathbf{S}_{mj}\cdot\mathbf{r}^{ij}_{nm})}{|\mathbf{R}^{ij}_{nm}|^3}, \quad (10)$$

with $D=(g\mu_B S)^2/a^3$, $\mathbf{R}^{ij}_{nm}$ being the vector linking two spins, measured in units of the lattice constant a, and $\mathbf{r}^{ij}_{nm}=\mathbf{R}^{ij}_{nm}/|\mathbf{R}^{ij}_{nm}|$. The strength of the dipolar coupling between two neighboring spins in $Gd_2Sn_2O_7$ is estimated as

$$E^d_{\rm n.n.} = \frac{(g\mu_B S)^2}{(a/2\sqrt{2})^3} = 16\sqrt{2}D = 0.605\ \text{K}, \quad (11)$$

where we have substituted $a=10.455$ Å for the lattice constant.[21] The parameter $E^d_{\rm n.n.}$ is three times smaller than the single-ion energy $D_a S^2 \sim 1.73$ K, but the dipolar interactions still play an important role due to their long-range nature. From now on we define dimensionless parameters $d_a=D_a/J=0.516$ and $d=D/JS^2=0.008$, normalizing all interactions to the exchange constant J and the excitation energies to JS.

Projecting Eq. (10) onto the four-sublattice magnetic structure ($\mathbf{S}_{ni}\equiv\mathbf{S}_i$) we obtain

$$\hat{\mathcal{H}}_{\rm dip} = \frac{1}{2}N\sum_{ij,\alpha\beta} S^\alpha_i S^\beta_j D^{\alpha\beta}_{ij}, \quad (12)$$

where the dipolar matrix is given by

$$D^{\alpha\beta}_{ij} = d\sum_m \frac{1}{|R^{ij}_{nm}|^3}[\delta_{\alpha\beta} - 3(\mathbf{r}^{ij}_{nm})^\alpha(\mathbf{r}^{ij}_{nm})^\beta]. \quad (13)$$

In a cubic crystal the diagonal matrix elements are $D^{\alpha\beta}_{ii}\sim\delta_{\alpha\beta}$ and drop out from the equations on the equilibrium spin configuration and on the energies of the $\mathbf{k}=0$ modes.

The dipolar sums are straightforwardly evaluated using Ewald's summation technique:[22]

$$D^{\alpha\beta}_{ij}/d = 16\pi\sum_{\mathbf{G}}{}' \frac{G^\alpha G^\beta}{G^2} e^{-G^2/4Q_c^2} e^{i\mathbf{G}\cdot(\boldsymbol{\rho}_i-\boldsymbol{\rho}_i)} + \sum_{\mathbf{R}}\Bigg\{ \text{erfc}(Q_c R_{ij}) \times\left[\frac{\delta_{\alpha\beta}}{R^3_{ij}} - \frac{3R^\alpha_{ij}R^\beta_{ij}}{R^5_{ij}}\right] - \frac{2Q_c}{\sqrt{\pi}R^2_{ij}} e^{-Q_c R^2_{ij}}\left[2Q_c^2 R^\alpha_{ij}R^\beta_{ij} - \delta_{\alpha\beta} + \frac{3R^\alpha_{ij}R^\beta_{ij}}{R^2_{ij}}\right]\Bigg\}, \quad (14)$$

where $Q_c\sim 1$ is an arbitrary cutoff, $\mathbf{G}$ is a reciprocal lattice vector, erfc(x) is the complementary error function, and $\mathbf{R}_{ij}=\mathbf{R}+\boldsymbol{\rho}_i-\boldsymbol{\rho}_j$, $\mathbf{R}$ being an fcc lattice vector. Summations in Eq. (14) are performed over all $\mathbf{R}$ and $\mathbf{G}$ excluding $\mathbf{G}=0$.

Cubic symmetry of the pyrochlore lattice leaves only three independent constants,

$$D^{xx}_{12}=D^{xx}_{34}=c_1,\quad D^{yy}_{12}=D^{zz}_{12}=D^{yy}_{34}=D^{zz}_{34}=c_2,$$

$$D^{yz}_{12}=D^{zy}_{12}=-D^{yz}_{34}=-D^{zy}_{34}=c_3,$$

$$D^{yy}_{13}=D^{yy}_{24}=c_1,\quad D^{xx}_{13}=D^{zz}_{13}=D^{xx}_{24}=D^{zz}_{24}=c_2,$$

$$D^{xz}_{13}=D^{zx}_{13}=-D^{xz}_{24}=-D^{zx}_{24}=c_3,$$

$$D^{zz}_{14}=D^{zz}_{23}=c_1,\quad D^{xx}_{14}=D^{yy}_{14}=D^{xx}_{23}=D^{yy}_{23}=c_2,$$

$$D^{xy}_{14}=D^{yx}_{14}=-D^{xy}_{23}=-D^{xy}_{23}=c_3. \quad (15)$$

Evaluating numerically the corresponding expressions [Eq. (14)] we find $c_1=17.92d=0.143$, $c_2=-34.09d=-0.273$, and $c_3=-57.84d=-0.463$.

The dipolar energy [Eq. (12)] can be used to compare the relative stability of different $\mathbf{q}=0$ magnetic structures. In particular, the dipolar contribution for the chiral spin-cross configuration [Eq. (1)], or the Palmer-Chalker state, is $E^d_1/NS^2=-2c_1+2c_3$. The alternative (nonchiral) spin-cross structure, which is realized in $Er_2Ti_2O_7$ (Ref. 23) and can be obtained from the chiral spin cross with $\mathbf{S}_2\to-\mathbf{S}_2$, $\mathbf{S}_3\to-\mathbf{S}_3$, has a higher dipolar energy $E^d_2/NS^2=2c_1-4c_2+2c_3$.

To calculate the effect of the dipolar interaction on the magnon spectra we transform again to the local spin frame in Eq. (12) and bosonize spin operators using Eq. (3). The dipolar matrix elements in the rotating coordinate system $\mathcal{D}^{\alpha\beta}_{ij}$ are expressed via the laboratory frame matrix $D^{\alpha\beta}_{ij}$ by

$$\mathcal{D}^{\alpha\beta}_{ij} = \hat{\mathbf{e}}^\mu_{i\alpha}\hat{\mathbf{e}}^\nu_{j\beta}D^{\mu\nu}_{ij}, \quad (16)$$

where $\hat{\mathbf{e}}_{i\alpha}$ are the local basis vectors [see Eq. (1)].

The obtained quadratic form of bosonic operators is

$$\hat{\mathcal{H}}^{(2)}_{\rm dip} = \sum_{\langle ij\rangle} -\mathcal{D}^{zz}_{ij}(a^\dagger_i a_i + a^\dagger_j a_j) + \frac{1}{2}(\mathcal{D}^{xx}_{ij}+\mathcal{D}^{yy}_{ij})(a^\dagger_i a_j + a^\dagger_j a_i) - \frac{i}{2}(\mathcal{D}^{xy}_{ij}+\mathcal{D}^{yx}_{ij})(a^\dagger_i a_j - a^\dagger_j a_i) + \frac{1}{2}(\mathcal{D}^{xx}_{ij}-\mathcal{D}^{yy}_{ij}) \times(a_i a_j + a^\dagger_i a^\dagger_j) - \frac{i}{2}(\mathcal{D}^{xy}_{ij}+\mathcal{D}^{yx}_{ij})(a_i a_j - a^\dagger_i a^\dagger_j). \quad (17)$$

The summation is performed over all sublattice pairs. Skipping the straightforward algebra behind the substitution [Eq. (16)] and the subsequent Bogoliubov transformation, we present the final results for the magnon energies. The two degenerate modes have the energy

$$\varepsilon^2_{2,3} = \frac{1}{3}[(2d_a-3c_3)(4+c_1+c_2) - 4c_3 d_a], \quad (18)$$

while the energies of the two other modes are given by (positive) roots of

$$3\varepsilon^4 - 2\varepsilon^2[6(c_1-c_2)(4+c_1+c_2) + (2d_a-3c_3) \times(8+5c_1-c_2-4c_3)] + 8(c_1-c_2)[2d_a-3c_3+2(c_1-c_2)] \times[(4+c_1+c_2)(2d_a-3c_3) - 4c_3 d_a] = 0. \quad (19)$$

The apparent discrepancy with the previous spin-wave calculation[13] for $Gd_2Sn_2O_7$ on the splitting between ε_2 and ε_3 can be traced back to an incorrect treatment of the single-ion term in that work. Indeed, the other paper of the same authors,[20] which takes into account only dipolar interactions, yielded a degenerate doublet for intermediate energy modes.

Restoring the scaling parameter JS and using the following values for the microscopic parameters, $J=0.27$ K, $d_a=0.516$, and $d=0.008$, we obtain for the gaps: $\Delta_1=1.24$ K, $\Delta_{2,3}=1.77$ K, and $\Delta_4=4.51$ K, which are already quite close to the experimentally measured values. An even better cor-

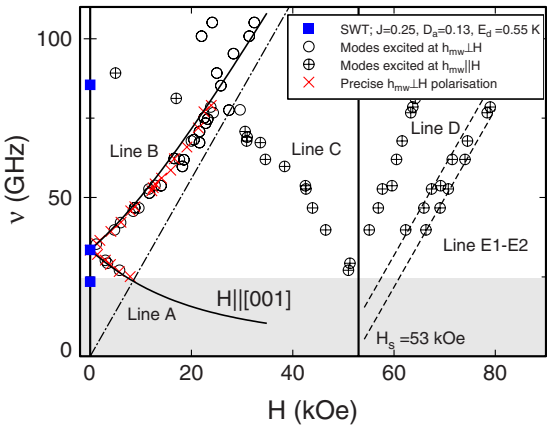

FIG. 4. (Color online) Frequency-field diagram of the resonance spectrum observed on a powder sample of $Gd_2Sn_2O_7$ at $T=0.45$ K; ○ and ⊕ correspond to the modes excited at $\mathbf{h}_{mw}\perp\mathbf{H}$ and $\mathbf{h}_{mw}\angle\mathbf{H}$, respectively; ■ mark the gap values calculated by the SWT; the solid lines represent the solution of Eq. (20) for a doublet mode with $H\|[001]$, the dashed lines are linear fits to the two components of spectral line E with $g=2$, and the dash-dotted line corresponds to a $g=2$ paramagnet. The transition to a spin-polarized phase at $H_s=53.0$ kOe is marked by a vertical line. The unreachable low-frequency range $\nu<25$ GHz is shaded in gray.

respondence between the theoretical and the experimental results for the three upper branches (shown by closed squares on the $H=0$ axis of Fig. 4) is achieved for a slightly modified set of microscopic constants: $J=0.25$ K, $D_a=0.13$ K ($d_a=0.52$), and $E_d=0.55$ K ($d=0.008$). The lowest gap in this case is equal to $\Delta_1=1.13$ K, which is close to the estimate obtained by fitting the specific-heat curve.

Comparing Eqs. (9), (18), and (19) and the corresponding estimates, we conclude that the dipolar interactions are essential in lifting the energy of the lowest branch Δ_1. On the other hand the gap of the two degenerate modes is predominantly determined by the single-ion anisotropy, while the highest gap Δ_4 has roughly equal contributions from the single-ion term and from the dipolar interactions. Thus, $Gd_2Sn_2O_7$ is a moderately anisotropic antiferromagnet, for which both the ground-state selection[16] and the spin dynamics are determined by a delicate balance of the nearest-neighbor exchange, the dipolar interactions, and the single-ion anisotropy.

V. DISCUSSION

In Sec. IV we have demonstrated a good agreement between the measured ESR spectrum and the spin-wave calculations performed in zero magnetic field. The two degenerate resonance branches correspond to a peculiar type of spin motion: oscillation of a spin plane with respect to two orthogonal in-plane axes. Such modes are excited by the perpendicular component of the microwave field $\mathbf{h}_{mw}\perp\mathbf{H}$ as is indeed observed for lines A and B.

Generalization of weak magnetic fields is straightforwardly done with the "hydrodynamic" approach,[24] which is valid once the exchange interactions are significantly stronger than magnetic anisotropies and field. Simple calculations analogous to those performed in Ref. 25 yield the following cubic equation for eigenfrequencies:

$$(\nu^2-\nu_1^2)(\nu^2-\nu_2^2)^2-\gamma^2\nu^2(\nu^2H^2-\nu_1^2H_\parallel^2-\nu_2^2H_\perp^2)=0, \tag{20}$$

where ν_1 and ν_2 are resonance frequencies in zero field, $H_\parallel$ and $H_\perp$ are magnetic field components with respect to the tetragonal axis, and $\gamma=g\mu_B/2\pi\hbar$ is the electronic gyromagnetic ratio ($g=2.0$). In gadolinium stannate the magnetic anisotropies are comparable to the nearest-neighbor exchange interaction. Moreover, the exchange structure is soft, i.e., infinitely degenerate, and the anisotropies play a decisive role in stabilizing the observed magnetic structure. This restricts applicability of the hydrodynamic theory, which is used here only to indicate a plausible behavior.

The field evolution of the spectrum is summarized on the frequency-field diagram presented in Fig. 4. The two degenerate modes appear to be split by the magnetic field into decreasing (line A) and increasing (line B) branches. The points in Fig. 4 mark the maximums of the ESR absorption which, for a powder sample, correspond to one of the outermost field orientations with respect to the crystal axes. The frequency-field dependence of these maximums for the two degenerate modes is satisfactorily fitted by formula (20) for $H\|[001]$ if one takes $h\nu_2=\Delta_{2,3}$ (solid lines in Fig. 4), while the third calculated branch is field independent and set to zero. When the orientation of the external field is changed from $H\|[001]\rightarrow H\perp[001]$, both branches shift to higher fields resulting in the overextended right wings of the absorption lines observed in the experiment. Hence, in spite of the "softness" of the exchange structure in a Heisenberg pyrochlore magnet, the spin plane oscillations are not strongly affected by quasilocal modes.

Third spectral mode C is excited only by a parallel microwave field component $h_{mw}\|H$, which indicates that it is not a uniform oscillation of the spin plane, but rather an antiphase motion of spins of the cross (in-plane or out-of plane). This mode should soften at the saturation point H_s (as observed in the experiment) and, on further increase in H, should develop a gap, which probably corresponds to increasing line D of the spectrum above H_s. The other two resonance branches (doublet line E) observed at $H>H_s$ have linear field dependences distinctive for quasilocal soft modes in the spin-polarized phase.[26] They were also observed in $Gd_2Ti_2O_7$, but unlike that case, the corresponding absorption lines are significantly broadened and less pronounced due to the distribution by magnetic field orientations in a powder sample. Nevertheless, one of them seems to have almost zero energy at $H=H_s$, which corresponds to the softening of one of the excitation branches at the antiferromagnetic wave vector $\mathbf{q}=0$ near the second-order transition. (The ordering wave vector in $Gd_2Ti_2O_7$ is different from $\mathbf{q}=0$, and therefore all ESR modes remain finite at $H=H_s$.) The spin-wave calculation of the high-field magnon spectrum and its comparison with the observed results can provide useful information on the parameters of the spin-Hamiltonian for the two pyrochlore materials.

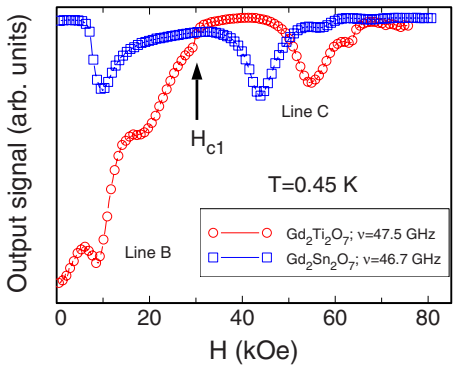

FIG. 5. (Color online) Absorption spectra recorded at nearly the same frequencies in $Gd_2Sn_2O_7$ powder sample (squares) and in $Gd_2Ti_2O_7$ single crystal at $H\|[111]$ (circles); the arrow marks the transition in $Gd_2Ti_2O_7$ at $H=H_{c1}\simeq 30$ kOe.

The measured resonance modes and their perfect agreement with the spin-wave calculations point at the conventional magnetic ordering in $Gd_2Sn_2O_7$ below 1 K. Note that an explanation of the persistent spin dynamics observed by the local probes[7–9] remains an open issue: gapped magnons with energies above 1 K cannot contribute to the muon spin relaxation in the 50 mK range. Still, properties of the sister material $Gd_2Ti_2O_7$ are strikingly different from the more conventional stannate. This concerns not only the difference in the low-temperature asymptotes for the specific heat[4,5] but also their ESR spectra as illustrated in Fig. 5. A typical absorption curve for $Gd_2Sn_2O_7$ consists of several spectral lines with almost zero background. In contrast, the recorded absorption curve for $Gd_2Ti_2O_7$ demonstrates a broad, intense nonresonant anomaly with a maximum in zero field. This additional absorption develops simultaneously with the main spectral lines below T_N, rapidly decreases with increasing magnetic field, and fully disappears stepwise at $H=H_{c1}\simeq 30$ kOe marked by an arrow in Fig. 5. The above findings provide evidence for additional "magnetic degrees of freedom" in the titanate, which exist down to low temperatures and are suppressed by an external magnetic field.

Additional low-energy excitations in $Gd_2Ti_2O_7$ may result from the complexity of magnetic ordering in this material. The neutron-diffraction experiments[2] suggest a multi-k spin structure in the titanate, which may also lead to multiple magnetic domains related to different combinations of $\mathbf{q}=(1/2,1/2,1/2)$ and equivalent wave vectors. Excitations in the domain walls and their pinning by crystal defects can produce additional low-temperature spin dynamics. Such a residual dynamics (i) should be absent in the $\mathbf{q}=0$ ground state of the stannate and (ii) should exhibit a significant sample dependence as was indeed found from the comparison of μSR data obtained on single crystal[5] and powder samples.[6] The low-field domain structure can be further eliminated by a magnetic field, which, for example, selects at $H>H_{c1}$ a unique ordering wave vector. An extra argument in favor of such a scenario is that the ESR spectrum of the titanate is significantly transformed at $H=H_{c1}$, becoming similar to the spectrum of the stannate.[25] Namely, line C of the spectrum, which is traced in the stannate in the whole field range $0<H<H_s$, appears in the titanate only at $H>H_{c1}$. High-field neutron-diffraction measurements in $Gd_2Ti_2O_7$ together with evolution of the low-T asymptote in the specific heat under magnetic field should provide a valuable check for the above scenario.

In summary, the study of the magnetic-resonance properties of the pyrochlore gadolinium stannate reveals three gapped resonance modes in the ordered phase, two of them being exactly degenerate at zero external magnetic field. The spin-wave theory (SWT), which takes into account the nearest-neighbor exchange, the single-ion anisotropy, and the dipolar interactions, demonstrates very good agreement with the experiment using known values of the microscopic magnetic parameters. The lowest gap value predicted by theory lies beyond the experimental frequency range and cannot be directly observed. Nevertheless, it roughly agrees with an estimate made from the exponential decrease in the low-temperature specific heat.

ACKNOWLEDGMENTS

The authors thank V. N. Glazkov and A. I. Smirnov for useful discussions. Work at the Kapitza Institute was supported by RFBR under Grant No. 07-02-00725 and by the Program of the President of Russian Federation. S.S.S. is grateful to INTAS for the financial support (Grant No. YSF 2004-83-3053) and to SPSMS/CEA-Grenoble for their hospitality during the joint research program. Likewise, M.E.Z. acknowledges warm reception at the Kapitza Institute.

[1] R. Moessner and J. T. Chalker, Phys. Rev. B **58**, 12049 (1998).
[2] J. R. Stewart, G. Ehlers, A. S. Wills, S. T. Bramwell, and J. S. Gardner, J. Phys.: Condens. Matter **16**, L321 (2004).
[3] A. S. Wills, M. E. Zhitomirsky, B. Canals, J.-P. Sanchez, P. Bonville, P. Dalmas de Réotier, and A. Yaouanc, J. Phys.: Condens. Matter **18**, L37 (2006).
[4] J. A. Quilliam, K. A. Ross, A. G. Del Maestro, M. J. P. Gingras, L. R. Corruccini, and J. B. Kycia, Phys. Rev. Lett. **99**, 097201 (2007).
[5] A. Yaouanc, P. Dalmas de Réotier, V. Glazkov, C. Marin, P. Bonville, J. A. Hodges, P. C. M. Gubbens, S. Sakarya, and C. Baines, Phys. Rev. Lett. **95**, 047203 (2005).
[6] S. R. Dunsiger, R. F. Kiefl, J. A. Chakhalian, J. E. Greedan, W. A. MacFarlane, R. I. Miller, G. D. Morris, A. N. Price, N. P. Raju, and J. E. Sonier, Phys. Rev. B **73**, 172418 (2006).
[7] E. Bertin, P. Bonville, J.-P. Bouchaud, J. A. Hodges, J. P. Sanchez, and P. Vulliet, Eur. Phys. J. B **27**, 347 (2002).
[8] P. Dalmas de Réotier, P. C. M. Gubbens, and A. Yaouanc, J. Phys.: Condens. Matter **16**, S4687 (2004).
[9] P. Bonville, J. A. Hodges, E. Bertin, J.-Ph. Bouchaud, P. Dalmas de Réotier, L.-P. Regnault, H. M. Rønnow, J.-P. Sanchez, S. Sosin, and A. Yaouanc, Hyperfine Interact. **156–157**, 103

(2004).
[10] S. S. Sosin, L. A. Prozorova, A. I. Smirnov, P. Bonville, G. Jasmin-Le Bras, and O. A. Petrenko, Phys. Rev. B **77**, 104424 (2008).
[11] P. Bonville, J. A. Hodges, M. Ocio, J.-P. Sanchez, P. Vulliet, S. Sosin, and D. Braithwaite, J. Phys.: Condens. Matter **15**, 7777 (2003).
[12] E. Janod, R. Calemczuk, J. Y. Henry, and C. Marcenat, Phys. Lett. A **205**, 105 (1995).
[13] A. Del Maestro and M. J. P. Gingras, Phys. Rev. B **76**, 064418 (2007).
[14] S. S. Sosin, A. I. Smirnov, L. A. Prozorova, O. A. Petrenko, M. E. Zhitomirsky, and J.-P. Sanchez, J. Magn. Magn. Mater. **310**, 1590 (2007).
[15] J. R. Stewart, J. S. Gardner, Y. Qiu, and G. Ehlers, Phys. Rev. B **78**, 132410 (2008).
[16] S. E. Palmer and J. T. Chalker, Phys. Rev. B **62**, 488 (2000).
[17] R. M. White, *Quantum Theory of Magnetism* (Springer, Berlin, 1983), p. 191.
[18] J. D. M. Champion and P. C. W. Holdsworth, J. Phys.: Condens. Matter **16**, S665 (2004).
[19] V. N. Glazkov, A. I. Smirnov, J.-P. Sanchez, A. Forget, D. Colson, and P. Bonville, J. Phys.: Condens. Matter **18**, 2285 (2006).
[20] A. G. del Maestro and M. J. P. Gingras, J. Phys.: Condens. Matter **16**, 3339 (2004).
[21] B. J. Kennedy, B. A. Hunter, and C. J. Howard, J. Solid State Chem. **130**, 58 (1997).
[22] P. P. Ewald, Ann. Phys. **64**, 253 (1921).
[23] J. D. M. Champion, M. J. Harris, P. C. W. Holdsworth, A. S. Wills, G. Balakrishnan, S. T. Bramwell, E. Cizmar, T. Fennell, J. S. Gardner, J. Lago, D. F. McMorrow, M. Orendac, A. Orendacova, D. McK. Paul, R. I. Smith, M. T. F. Telling, and A. Wildes, Phys. Rev. B **68**, 020401(R) (2003).
[24] A. F. Andreev and V. I. Marchenko, Sov. Phys. Usp. **23**, 21 (1980).
[25] S. S. Sosin, A. I. Smirnov, L. A. Prozorova, G. Balakrishnan, and M. E. Zhitomirsky, Phys. Rev. B **73**, 212402 (2006).
[26] M. E. Zhitomirsky and H. Tsunetsugu, Phys. Rev. B **70**, 100403(R) (2004).